# Molecular Dynamics Simulation of Main Chain Liquid Crystalline Polymers

**Alexey V. Lyulin,† Muataz S. Al-Barwani, and Michael P. Allen***

*H. H. Wills Physics Laboratory, University of Bristol, Royal Fort, Tyndall Avenue, Bristol BS8 1TL, U.K.*

**Mark R. Wilson**

*Department of Chemistry, University of Durham, South Road, Durham DH1 3LE, U.K.*

**Igor Neelov**

*Polymer Chemistry Department, Helsinki University, PB 55, A. I. Virtasen Aukio 1, FIN-00014, HY, Helsinki, Finland*

**Nicholas K. Allsopp**

*High Performance Computing Centre, Southampton University, Highfield, Southampton SO17 1BJ, U.K.*

*Received July 22, 1997; Revised Manuscript Received April 21, 1998*

ABSTRACT: Molecular dynamics simulations of a model main-chain liquid crystalline polymer (LCP) and of a low molecular weight analogue have been carried out using an efficient parallel algorithm. A main-chain LCP is formed with the help of Gay−Berne mesogenic units connected to each other through flexible methylene spacers. We have studied the effect of varying the spacer length, and have examined the region of the isotropic-liquid crystalline transition. Our preliminary results indicate that liquid crystalline ordering may occur spontaneously on lowering the temperature, and that odd−even dependences of thermodynamic properties on spacer length occur, in agreement with existing experiments. Local orientational time correlation functions, as well as local translational mobility, have been studied both for the mesogenic elements and the bonds in the flexible spacer. The anisotropy of both orientational and translational local dynamical properties have been compared with theoretical predictions and with Brownian dynamics results for a freely jointed chain in a liquid crystalline orienting field.

## I. Introduction

Theoretical and experimental studies of liquid crystalline (LC) polymers have been a popular field of investigation for the last two decades. Considerable progress has already been made in understanding the behavior of these systems, though many effects have yet to be explained. Recently, advanced simulation techniques have been applied to the study of the LC state of matter by making use of molecular dynamics (MD) and Monte Carlo (MC) methods. At present these investigations have mainly been devoted to low molecular weight compounds.[1−8] However, recently some progress has been made in extending these simulations to polymer liquid crystal systems. Computer simulations of main-chain LC polymers by the method of Brownian dynamics (BD) on the basis of a rather simplified model have been performed.[9,10] In these works it is supposed that the dynamics of chain elements in a nematic LC polymer can be considered as the motion of a single chain in a viscous medium under the influence of an anisotropic LC field[11,12]

$$U(\theta) = -U_0 \cos^2 \theta \tag{1}$$

where $\theta$ is the angle between the long axis of a mesogenic element and the direction of the external LC field, and $U_0$ is the magnitude of the potential barrier. This barrier separates two stable states corresponding to $\theta = 0$ and $\theta = \pi$. In ref 10, BD simulation of a freely jointed chain with rigid bonds and without excluded-volume or hydrodynamical interactions was carried out. The LC field of eq 1 was taken to affect each bond, modeling the situation in a linear polymer LC with mesogenic groups in the main chain. The simulation algorithm involved the solution of Langevin's equations in the large friction case for the chain junctions in the presence of the external field of eq 1. It has to be emphasized that, in this model, mesogenic elements are directly connected to each other: no flexible spacers were considered explicitly.

The main results of ref 10 could be summarized as follows: the presence of the LC field leads to anisotropy of (i) the conformational properties and (ii) the orientational mobility of the polymer chain. As a measure of the first effect, the projection of the mean-square end-to-end distance on the direction of the field $\langle h_{\parallel}^2 \rangle$, increases, while the perpendicular projection $\langle h_{\perp}^2 \rangle$, decreases, with increasing magnitude of the field $U_0$ and, correspondingly, with increasing order parameter of chain links $S = {}^3/_2\langle \cos^2 \theta - {}^1/_3 \rangle$.

To investigate the orientational mobility of mesogenic elements, the autocorrelation functions

$$P_{\parallel}^{(1)}(t) = \frac{\langle \cos \theta(0) \cos \theta(t) \rangle}{\langle \cos^2 \theta \rangle}$$

$$P_{\perp}^{(1)}(t) = \frac{\langle \cos \gamma(0) \cos \gamma(t) \rangle}{\langle \cos^2 \gamma \rangle} \tag{2}$$

* Author for correspondence. E-mail m.p.allen@bristol.ac.uk.
† Permanent address: Institute of Macromolecular Compounds, Russian Academy of Sciences, 199004 St. Petersburg, Russia. E-mail alex@imc.macro.ru.

S0024-9297(97)01105-4 CCC: $15.00 
Published on Web 06/19/1998

were calculated. Here $\theta$ and $\gamma$ are the angles made by the long axis of the mesogenic element with the field direction, and with a perpendicular direction, respectively. The decay of each of these functions is characterized by a corresponding relaxation time, $\tau_{||}^{(1)}$ and $\tau_{\perp}^{(1)}$, respectively. In the LC state, there is anisotropy of local orientational mobility of the mesogenic elements, namely, $\tau_{||}^{(1)}$ increases while $\tau_{\perp}^{(1)}$ decreases with increase of ordering. As suggested in ref 10, this anisotropy is due to two main mechanisms of orientational motion of the mesogenic elements, both dependent on the LC field: (a) motions within the potential well and (b) transitions over the potential barrier $U_0$.

The first mechanism is responsible for the relaxation of the function $P_{\perp}^{(1)}(t)$. The dependence of $\tau_{\perp}^{(1)}$ on $S$ obtained for mesogenic units included in a chain was found to be similar to that for a single dumbbell (two centers of viscous friction connected by a rigid rod) in the same nematic field and was consistent with the analytical formula[13]

$$\tau_{\perp}^{(1)} = \frac{(1 - S)}{(2 + S)} D_{\mathrm{r}}^{-1} \tag{3}$$

where $D_{\mathrm{r}}$ is the rotational diffusion coefficient for a rigid dumbbell in the absence of an ordering field.

The second mechanism is responsible for the relaxation of the function $P_{||}^{(1)}(t)$. It is possible to estimate analytically the transition time $\tau_{\mathrm{t}}$ over the potential barrier $U_0$ for a single dumbbell, using the approach suggested by Lyulin et al.,[14] and this expression also describes the behavior of $\tau_{||}^{(1)}$ effectively:

$$\tau_{||}^{(1)} = \tau_{\mathrm{t}} = C D_{\mathrm{r}}^{-1} (U_0/k_{\mathrm{B}}T)^{-3/2} \exp(U_0/k_{\mathrm{B}}T) \tag{4}$$

($C$ is a numerical constant). The same expression should apply to any rigid mesogenic group not included in the polymer chain. This dependence of relaxation time on the external field (and order parameter) is weaker than predicted by the well-known Kramers theory[15]

$$\tau_{||}^{(1)} = \tau_{\mathrm{t}} = C D_{\mathrm{r}}^{-1} (U_0/k_{\mathrm{B}}T)^{-1} \exp(U_0/k_{\mathrm{B}}T) \tag{5}$$

As shown in ref 14, this difference arises because of the spatial character of orientational diffusion in contrast to the planar case considered by Kramers. In ref 14, the conclusion is drawn that the relaxation of the function $P_{||}^{(1)}(t)$ is actually determined by the transitions over the barrier $U_0$.

In the present paper, MD simulation of a many-particle heterogenic model of main-chain LC polymers has been carried out. In our model, rigid elongated mesogenic units, interacting with each other through an anisotropic pair potential[16] are connected by flexible methylene spacers; we examine several different spacer lengths. Both conformational and local dynamical properties of the elements of the polymer chain (mesogenic units and bonds in the spacer) have been investigated in the region of the isotropic liquid crystalline transition. The goal of this work is the study of conformational and dynamical mobility and anisotropy of the system in possible LC phases, and the comparison of results with theoretical predictions and BD simulation results for the simplified models described above. The advantage of the current approach is that no assumptions need be made regarding the behavior of single chains in an effective potential such as eq 1: interchain correlations giving rise to the effects modeled in this approximate way are all included exactly. In addition, the effects of spacer mobility are properly included in the simulation, which also allows us to look at the effects of liquid crystalline ordering on conformational and dynamical properties of the spacer bonds.

**Table 1. Transition Temperature to the Mesomorphic State $T_m$ and Isotropization Temperature $T_i$, Both in degrees Celsius, for Members of the Series PE1/n**

| $n$ | $T_m$ | $T_i$ |
|---|---|---|
| 5 | 178 | 310 |
| 6 | 238 | 347 |
| 7 | 180 | 312 |
| 9 | 180 | 282 |
| 10 | 224 | 288 |

## II. Model and Algorithm

Our molecular model is intended to mimic, roughly, the structure of the LC main-chain polyester PE1/n. The monomeric unit of these polymers is

$$\ldots -\mathrm{COO}-\mathrm{C_6H_4}-\mathrm{COO}-\mathrm{C_6H_4}-\mathrm{COO}-\mathrm{C_6H_4}-\mathrm{COO}-(\mathrm{CH_2})_n- \ldots$$

and typically $5 \le n \le 10$. The synthesis of these polymers is described elsewhere.[17] The series exhibits odd−even effects in the dependence on $n$ of the transition temperature to the mesomorphic state $T_m$, as well as the isotropization temperature $T_i$, as indicated in Table 1. X-ray investigations of these polymers[18−20] reveal that the polymers of the even series form smectic-A phases (molecular axes normal to the smectic layers) while the polymers of the odd series form smectic-C phases (molecular axes inclined with respect to the layer normals).

We represent a single polymer chain as a sequence of elongated mesogenic elements connected to each other by flexible spacers. Each such element is taken to be a Gay−Berne (GB) ellipsoid[16] with geometrical parameters and mass close to that for the mesogenic element in PE1/n. The interaction energy between a pair of mesogenic elements in our model is given by the Gay−Berne potential

$$v(\mathbf{e}_i, \mathbf{e}_j, \mathbf{r}_{ij}) = 4\epsilon(\mathbf{e}_i, \mathbf{e}_j, \hat{\mathbf{r}}_{ij})\{\rho^{-12} - \rho^{-6}\} \tag{6}$$

where

$$\rho = \frac{r_{ij} - \sigma(\mathbf{e}_i, \mathbf{e}_j, \hat{\mathbf{r}}_{ij}) + \sigma_0}{\sigma_0} \tag{7}$$

The distance function $\sigma$ depends on the relative orientations of the elements and the unit vector $\hat{\mathbf{r}}_{ij} = \mathbf{r}_{ij}/r_{ij}$ between particles $i$ and $j$

$$\sigma(\mathbf{e}_i, \mathbf{e}_j, \hat{\mathbf{r}}_{ij}) = \sigma_0 \left\{ 1 - \frac{\chi}{2} \left[ \frac{(\mathbf{e}_i \cdot \hat{\mathbf{r}}_{ij} + \mathbf{e}_j \cdot \hat{\mathbf{r}}_{ij})^2}{1 + \chi \mathbf{e}_i \cdot \mathbf{e}_j} + \frac{(\mathbf{e}_i \cdot \hat{\mathbf{r}}_{ij} - \mathbf{e}_j \cdot \hat{\mathbf{r}}_{ij})^2}{1 - \chi \mathbf{e}_i \cdot \mathbf{e}_j} \right] \right\}^{-1/2} \tag{8}$$

where $\chi = (\kappa^2 - 1)/(\kappa^2 + 1)$ is the shape anisotropy parameter $\kappa = \sigma_{\mathrm{ee}}/\sigma_{\mathrm{ss}}$, $\sigma_{\mathrm{ss}} = \sigma_0$ is the side-by-side diameter, and $\sigma_{\mathrm{ee}}$ is the end-to-end diameter of the Gay−

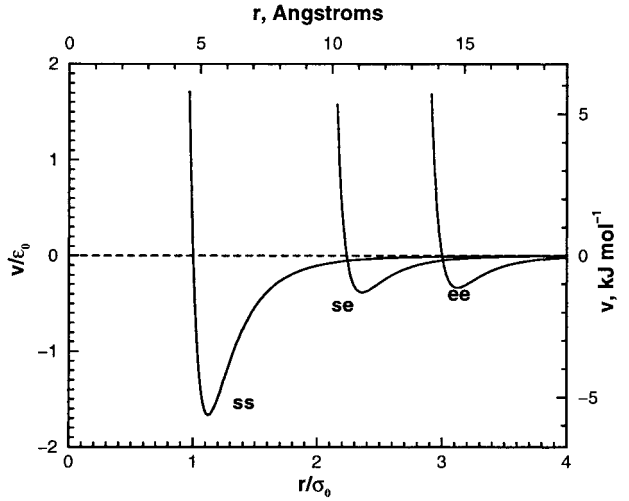


**Figure 1.** Gay−Berne potential for three different orientations: side-by-side (ss), end-to-end (ee) and side-to-end (se). The axes are labeled in "reduced units" based on the parameters $\sigma_0$, $\epsilon_0$, and in real units based on our chosen values for these parameters.

Berne ellipsoid. The strength of the interactions $\epsilon$ also depends on the relative orientations of the two mesogenic elements and takes the form

$$\epsilon(\mathbf{e}_i, \mathbf{e}_j, \hat{\mathbf{r}}_{ij}) = \epsilon_0[\epsilon'(\mathbf{e}_i, \mathbf{e}_j, \hat{\mathbf{r}}_{ij})]^{\mu} \times [\epsilon''(\mathbf{e}_i, \mathbf{e}_j)]^{\nu}$$

$$\epsilon'(\mathbf{e}_i, \mathbf{e}_j, \hat{\mathbf{r}}_{ij}) = 1 - \frac{\chi'}{2}\left[\frac{(\mathbf{e}_i\cdot\hat{\mathbf{r}}_{ij} + \mathbf{e}_j\cdot\hat{\mathbf{r}}_{ij})^2}{1 + \chi'\mathbf{e}_i\cdot\mathbf{e}_j} + \frac{(\mathbf{e}_i\cdot\hat{\mathbf{r}}_{ij} - \mathbf{e}_j\cdot\hat{\mathbf{r}}_{ij})^2}{1 - \chi'\mathbf{e}_i\cdot\mathbf{e}_j}\right]$$

$$\epsilon''(\mathbf{e}_i, \mathbf{e}_j) = [1 - \chi^2(\mathbf{e}_i\cdot\mathbf{e}_j)^2]^{-1/2} \qquad (9)$$

where $\chi' = (\kappa'^{1/\mu} - 1)/(\kappa'^{1/\mu} + 1)$ and $\kappa' = \epsilon_{ss}/\epsilon_{ee}$. $\epsilon_{ss}$ is the minimum of the potential for a pair of parallel units placed side-by-side, and $\epsilon_{ee}$ is the minimum for a pair of parallel units placed end-to-end. The parameters $\mu$ and $\nu$ were fixed to the values $\mu = 2$ and $\nu = 1$ as in the original paper.[16] We took $\sigma_0 = 4.721$ Å, $\epsilon_0 = 3.38$ kJ/mol, $\kappa = 3$, and $\kappa' = 5$. The potential for different orientations of the two Gay−Berne particles is illustrated in Figure 1.

We represent a spacer connecting two Gay−Berne units as a sequence of united atoms, each modelling a methylene group, and interacting with each other through the usual Lennard-Jones potential with parameters $\epsilon = 0.6$ kJ/mol and $\sigma = 3.923$ Å. The form used for the united atom/Gay−Berne interaction is taken from the work of Cleaver et al.,[21] who derive a generalized potential for two unlike Gay−Berne particles. In eq 37 of ref 21, we use a value for $\epsilon_0 = 1.42$ kJ/mol for the minimum well depth of the united atom/Gay−Berne interaction, which is the geometric mean of the Lennard-Jones and Gay−Berne well depths. The separation at which the interaction energy is zero $\sigma_0$ (eq 20 of ref 21) is given a value of 4.117 Å.

Valence bond lengths in the methylene spacer are constrained to $l_1 = 1.53$ Å (for methylene-methylene bonds) and $l_2 = 6.37$ Å (for methylene−GB bonds, this being measured to the center of the GB unit). Valence angles are specified with the help of a simple harmonic bending potential

$$U_b = \frac{1}{2}K(\alpha - \alpha^{(0)})^2 \qquad (10)$$

Here $K = 520.37$ kJ/mol, and $\alpha^{(0)}$ is the equilibrium bond angle. We take $\alpha^{(0)} = 124°58'$ for the angle at the end of the spacer, $\alpha^{(0)} = 109°28'$ for the angle inside the spacer, and $\alpha^{(0)} = 0$ to specify the harmonic potential between the GB unit and the first rigid bond in the spacer. This last term prevents large distortions of the mesogenic element from the configuration in which it is directed along the valence bond. Torsional interactions for dihedral angles in the spacer are described through the Ryckaert−Bellemans potential.[22]

In this paper we consider systems of 64 polymer chains of degree of polymerization $M = 10$ (which is a typical chain length for the polymers synthesized in ref 17). We consider various lengths of flexible spacer: $m = 5-8$. In all cases, the temperature was varied from 500 K down to 350 K. We started each series of simulations from an initial low-density lattice configuration. Then, a combination of constant-temperature MD and constant-pressure ($P = 0$) MC was carried out to equilibrate the system at the highest temperature. Equations of motion were solved using a leap-frog algorithm described in detail in ref 23. The time step was 2 fs in all cases. Translational and rotational ordering were rapidly lost, but a substantial period was allowed to ensure configurational equilibrium to be achieved. Each successive run was equilibrated from the final configuration at the next highest temperature. It should be emphasized that, to do this, in all cases considered here, equilibration took 6−16 ns, depending on temperature and size of system. These runs are long by the normal standards of molecular simulation. Equilibration was controlled by monitoring fluctuations of the total energy, the total kinetic energy, and the translational temperature. After equilibration, standard constant-NVE MD was performed. The length of production runs varied from 500 ps to 1 ns for each state point. All production runs, and most of the equilibration runs, were performed on an IBM SP2 supercomputer using a parallel algorithm specially developed for this problem. The algorithm used was based on a replicated data technique for a collection of anisotropic particles.[24] Following accumulation of our initial results, further runs were carried out at selected state points to check equilibration, using both IBM SP2 and Cray T3E supercomputers (see next section).

To check the code, and to have a reference point, MD simulations of a liquid of 512 *unconnected* GB molecules were also carried out at zero pressure and different temperatures in the vicinity of the transition between isotropic and liquid crystalline phases. This is a well-studied model of small-molecule liquid crystals.[3,7] The orientational order in the fluid was quantified by diagonalizing the order tensor, defined as

$$Q_{\alpha\beta} = \frac{1}{N}\sum_{i=1}^{N}\frac{1}{2}(3u_{i\alpha}u_{i\beta} - \delta_{\alpha\beta}) \qquad (11)$$

where $u_{i\alpha}$ is the $\alpha$ component ($\alpha = x, y, z$) of the unit vector along the long axis of a Gay−Berne unit $i$, or a bond in a flexible spacer, and $N$ is the corresponding number of such units; $\delta_{\alpha\beta}$ is the Kronecker delta. The order parameter $S$ was defined separately for GB units and spacer bonds, as the ensemble average of the largest eigenvalue of the order tensor, and the director $\hat{\mathbf{n}}$ (the

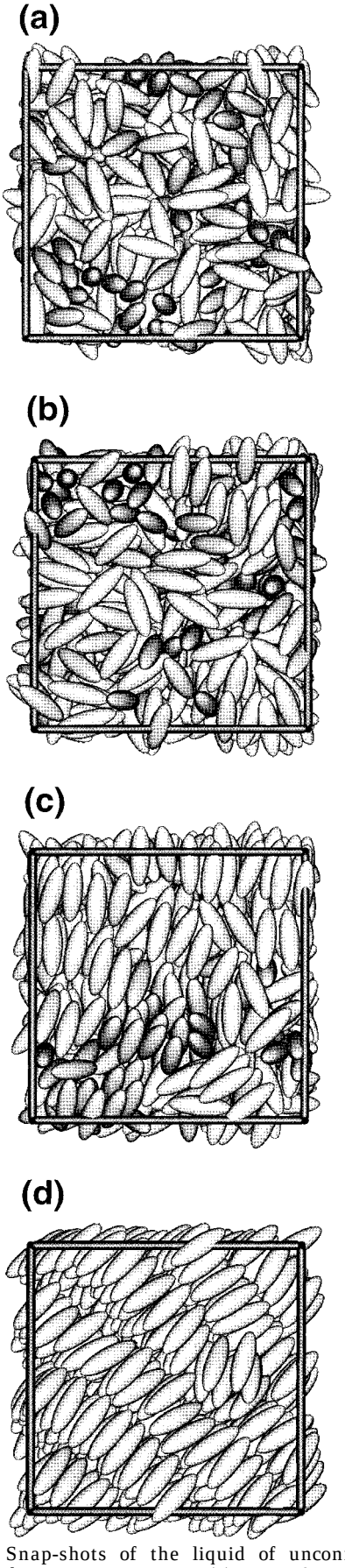


**Figure 2.** Snap-shots of the liquid of unconnected GB ellipsoids in the transition region: (a) $T = 170$ K, (b) $T = 165$ K, (c) $T = 162$ K, (d) $T = 160$ K.

average direction of alignment) as its corresponding eigenvector.

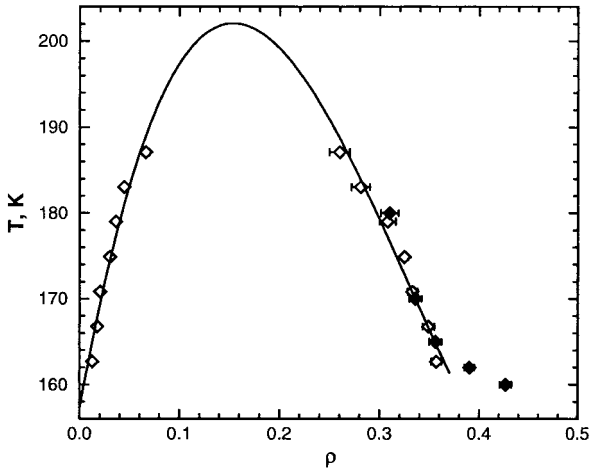


**Figure 3.** Liquid−vapor coexistence curve for the GB fluid in the temperature−density (volume fraction) plane. Open symbols with error bars represent vapor and liquid densities as obtained in ref 3 by using the Gibbs ensemble Monte Carlo technique. The line is a cubic fit to guide the eye. Filled symbols with error bars correspond to the liquid densities at zero pressure from the current work. The lowest two temperatures correspond to the smectic phase and the higher temperatures to isotropic liquid.

### III. Statistical and Structural Properties

Decreasing the temperature leads to spontaneous orientational ordering in both the low molecular weight system and the polymer melts. Typical snapshots for the low molecular weight LC (unconnected GB ellipsoids) in the region of the isotropic to liquid crystalline phase transition are presented in Figure 2. In ref 3 this system was studied by Gibbs ensemble Monte Carlo. According to ref 3, for this system, a spontaneous phase transition to the smectic-B phase has been established.

In Figure 3, the liquid branch of the liquid−vapor coexistence curve obtained in ref 3 is well reproduced in our zero-pressure simulations.

The high-density data shown in Figure 3 corresponds to the smectic-B phase. It should be noted that liquid−vapor coexistence occurs at quite low pressures for the temperatures studied here, so we would expect this to be a reasonable comparison.

Two snapshots of the polymer melt with spacer length $m = 6$ in the isotropic and LC states are shown in Figure 4. Visual inspection, and spatial correlation functions to be described shortly, suggest that the LC phase seen for the polymers is nematic; no indication of a smectic phase has been found at the temperatures studied. The orientational order parameters, for mesogenic GB units in both low molecular weight and polymeric systems, are reported in Figure 5. $S$ is higher for polymers with an even number of bonds in the spacer than that for systems with an odd number of bonds at the same temperature. The maximum value of the order parameter, $S = 0.48$, has been obtained for the polymer with spacer length $m = 6$ at $T = 350$ K. It should be emphasized that considerable time was allowed to grow this anisotropic system from the isotropic melt: more than 14 ns ($7 \times 10^6$ steps) to equilibrate the $T = 370$ K system from $T = 400$ K and a further 14 ns to cool this system to the next temperature down, $T = 350$ K. It is essential to approach the ordered phase by cooling in this way: to have confidence in its thermodynamic stability relative to the isotropic phase. Moreover, the

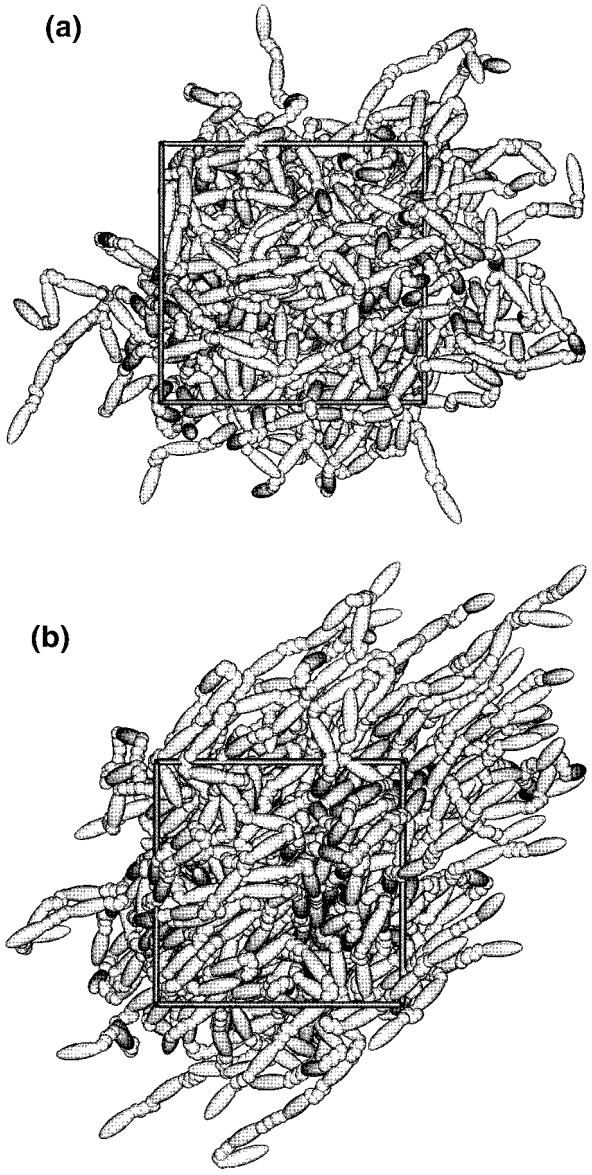


**Figure 4.** Snapshots of a polymer system with spacer length $m = 6$: (a) in the isotropic state, $T = 500$ K; (b) in the LC state, $T = 350$ K.

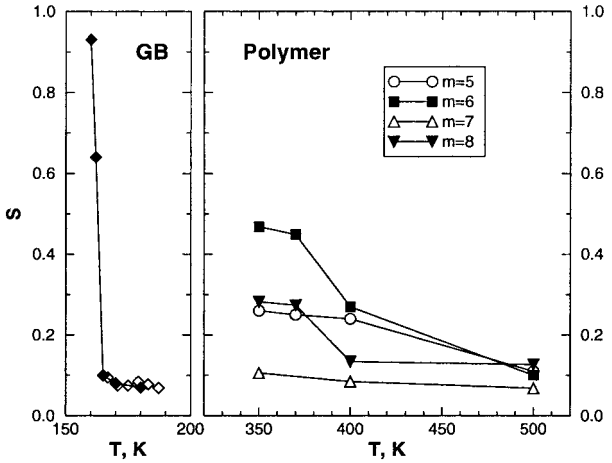


**Figure 5.** Orientational order parameter as a function of temperature. We show results for small-molecule Gay−Berne system determined by Gibbs ensemble Monte Carlo simulation[3] (open symbols) and in this work (filled symbols). We show order parameters of the Gay−Berne units in the polymers with spacer lengths: $m = 5$ (circles), $m = 6$ (squares), $m = 7$ (up triangles), $m = 8$ (down triangles). Odd−even effects are highlighted by using filled symbols for even $m$ and open symbols for odd $m$.

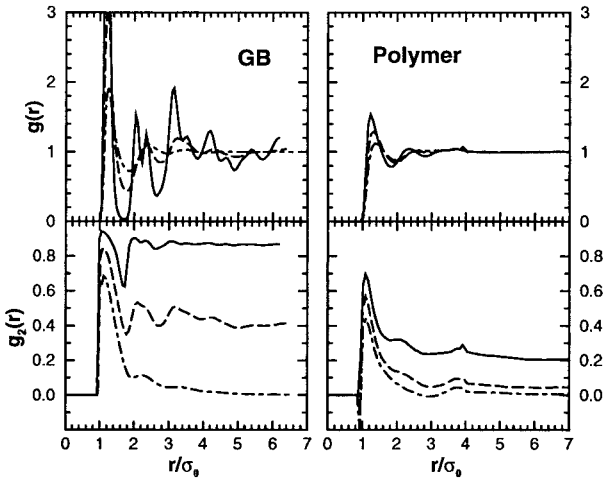


**Figure 6.** Pair distribution function $g(r)$ and second-rank orientational distribution function $g_2(r)$, for small-molecule GB system and for polymer with $m = 6$, at various temperatures in the isotropic and LC phases. For the GB system we show results for $T = 160$ K (solid line), 162 K (dashed line), 165 K (dot−dash line); the curves for $T = 170$ K are very similar to $T = 165$ K. For the polymer with $m = 6$ we show results for $T = 350$ K (solid line), 400 K (dashed line), 500 K (dot−dash line); the curves for $T = 370$ K are very similar to $T = 350$ K.

equilibrium orientational order parameter seems to change over a wide range of temperature (several tens of Kelvin). By contrast, for the low molecular weight GB system, the transition to the smectic phase is rather sharp and occurs within a temperature range of a few Kelvin (see Figure 5).

To check equilibration of the system, the runs for $m = 5$ at $T = 350$, 370 and 400 K and the run for $m = 6$ at $T = 400$ K, were all extended by a further 8 ns: the changes in the orientational order parameter in each case were very small. For $m = 7$, extending the runs at $T = 350$, 400 and 500 K by 1.2 ns also showed no changes, in that the system remained disordered.

The radial pair distribution function $g(r)$ and the second-rank orientational correlation function $g_2(r)$

$$g_2(r) = \langle P_2(\cos \gamma_{ij}(r)) \rangle \tag{12}$$

have been measured for GB units in the polymer and low molecular weight systems (see Figure 6). Here $\gamma_{ij}(r)$ denotes the angle between the long axes of a pair of units $i$ and $j$ lying in a narrow shell of center-of-mass separations $r_{ij} \approx r$. For the low molecular weight system in the isotropic phase, $g_2(r)$ decays monotonically to a value of zero for sufficiently large separations. In the LC phase, this limit is nonzero and equal to the square of the order parameter, $S^2$. Strong oscillations in $g(r)$ at the lower temperatures reflect the formation of a smectic phase. The principal peak in $g(r)$ for the small-molecule system at $T = 160$ K is $g(r) \approx 7$ (off scale in the figure). In the polymer system, the asymptotic large-$r$ value of $g_2(r)$ is again equal to $S^2$. In contrast with the GB system, in the liquid crystal phase, there is no sign of long-range positional order (i.e., the system appears to have formed a nematic, not a smectic, phase). $g_2(r)$ varies more smoothly at shorter distances (see Figure 6). The principal peak (and at the lowest temperature a secondary shoulder at $r/\sigma_0 \approx 2$) reflects

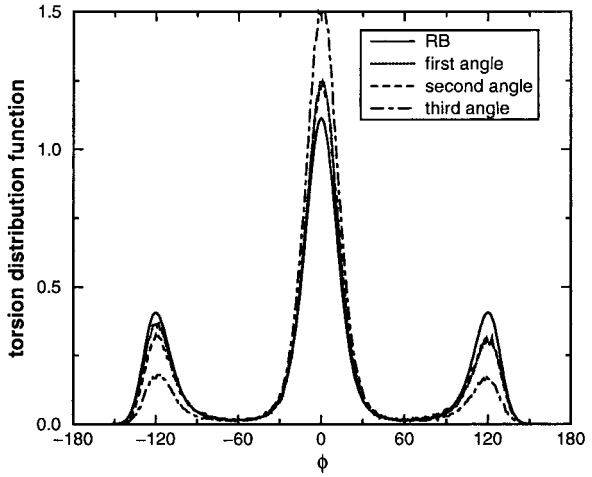


**Figure 7.** Torsional distribution functions (arbitrary units) for different dihedral angles in the spacer, for system $m = 6$: first angle (dotted line), second angle (dashed line), third angle (dot−dash line). For comparison, we also show (solid line) the theoretical distribution function from the Ryckaert−Bellemans torsional potential.

**Table 2. Percentage of *trans* and *gauche* Conformers for Different Dihedral Angles along Flexible Spacer[a]**

| | $\phi_1$ | | $\phi_2$ | | $\phi_3$ | |
|---|---|---|---|---|---|---|
| $T$ | % gauche | % trans | % gauche | % trans | % gauche | % trans |
| 350 | 16.2 | 67.8 | 16.2 | 67.9 | 9 | 82 |
| 370 | 16.7 | 66.8 | 16.7 | 66.7 | 10.1 | 80 |
| 400 | 19.7 | 60.7 | 17.9 | 64.2 | 12.2 | 72.6 |
| 500 | 22.9 | 54.2 | 20.2 | 59.7 | 14.3 | 71.5 |

[a] $\phi_1$ (nearest to mesogenic unit), $\phi_2$ (next-nearest) and $\phi_3$ (furthest), at different temperatures for the system $m = 6$.

some short-range side-by-side ordering. A small maximum at $r/\sigma_0 \approx 4$ reflects the strong *intramolecular* correlations. The $g(r)$ results for all the other spacer lengths $m$ are similar to the case $m = 6$: there is no indication of long-range positional order at the temperatures studied here. Also, the degree of orientational order is quite low, except for $m = 6$ as outlined above, and for $m = 8$ at the lowest temperature studied.

We have investigated the distribution of different conformers as a function of bond position along the spacer. Increasing the distance along the spacer from the GB unit, the proportion of *trans* conformers increases and the proportion of *gauche* conformers decreases, for all the systems studied here. In Figure 7 we plot the torsional distribution functions for the system with spacer length $m = 6$ in the LC state at $T =$ 350 K. Increasing the temperature leads to an increasing percentage of *gauche* conformers and a corresponding decrease in the fraction of *trans* conformers, for all bonds of the spacer (see Table 2). This is because *trans* conformations of spacer bonds favor parallel orientation of neighboring mesogenic elements. The rather small proportion of *gauche* conformers in the middle of the spacer reflects the highly disfavored crossed conformation of two neighboring mesogenic elements.

Ordering of the GB units induces some ordering in the spacers, as also observed in ref 25. We see an odd−even effect within the spacers for all the polymer LC systems: the order parameter for "even" (i.e., second, fourth, etc.) bonds is much higher than that for "odd" bonds (see Figure 8). This fact can be explained by simple geometry: in the LC state, when the elongated

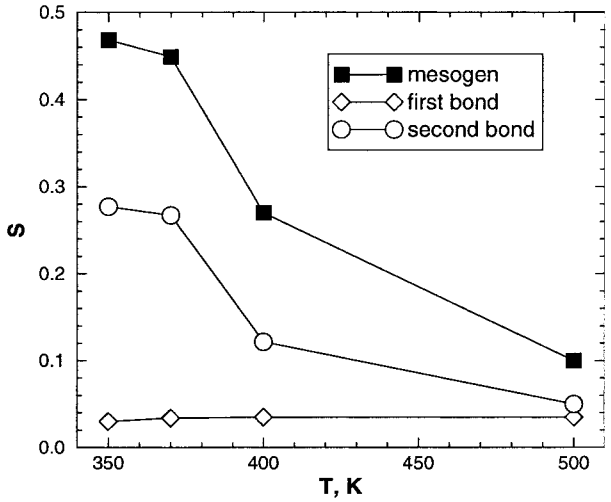


**Figure 8.** Temperature dependence of order parameter $S$ in mesogenic GB unit and spacer bonds for chains with spacer length $m = 6$.

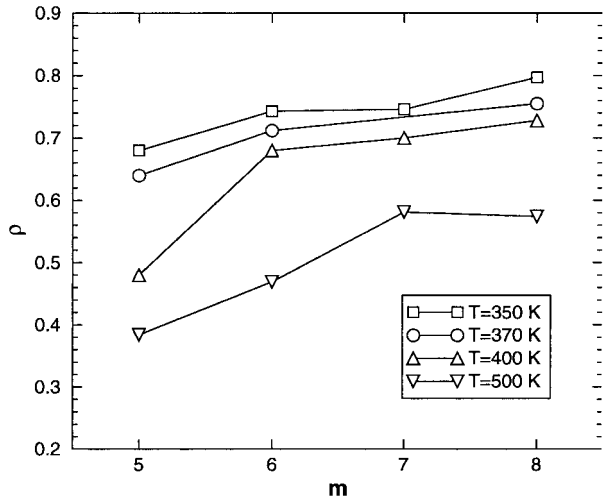


**Figure 9.** Equilibrium density (volume fraction) as a function of spacer length at different temperatures: $T = 350$ K (squares), $T = 370$ K (circles), $T = 400$ K (up triangles), $T =$ 500 K (down triangles).

*trans* conformation is favored, "even" bonds in the spacer are arranged mostly parallel to the nearest GB unit in the chain, and so the order parameter for these bonds is higher than for "odd" bonds.

There is further evidence of an odd-even effect in the equation of state. The equilibrium density at given $T$ and $P = 0$ is higher for even $m$, and lower for odd $m$, than would be expected on the basis of a smooth trend (see Figure 9). This reflects the fact that even-$m$ chains pack together more efficiently. Also, changing the temperature for the polymer system is accompanied by a large change in the density. Because the transition to the ordered phase seems to occur over a wide range of temperature, the accompanying density change is also quite large. For the $m = 6$ system, lowering $T$ from 500 to 400 K changes the order parameter from $S \approx 0.1$ to $S \approx 0.2$, while the density increases by ≈50%. A further reduction to 370 K increases the order to $S \approx 0.45$, and the density increases by ≈2%; a further density rise of ≈7% occurs as the order rises to $S = 0.48$ at $T = 350$ K. By comparison, for the low molecular weight system, a similar change of order parameter occurs over a much smaller temperature range and is accompanied by a much smaller density increase (less than 10%). This

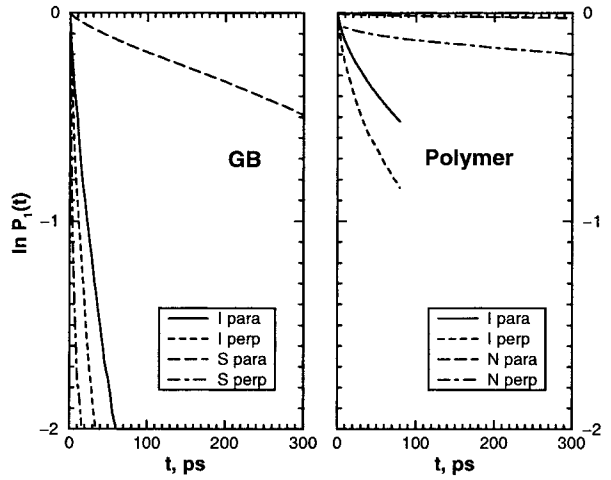


**Figure 10.** Orientational parallel and perpendicular correlation functions for small-molecule Gay−Berne system and mesogenic GB elements in polymer chain, spacer length $m = 6$. Results for both isotropic (I) and LC smectic (S) or nematic (N) phases are shown.

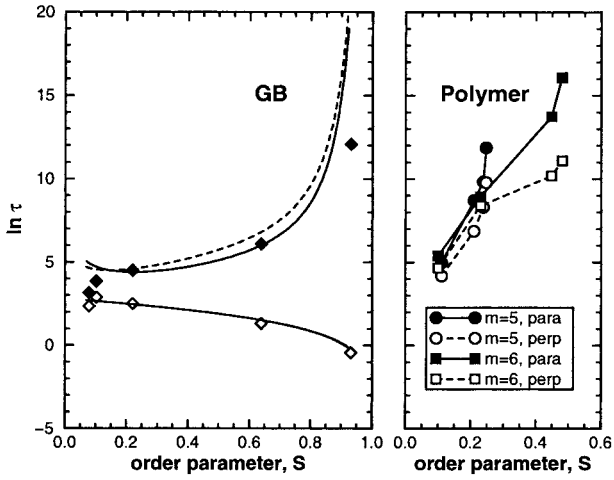


**Figure 11.** Anisotropy of orientational mobility for low-molecular weight Gay−Berne system and for mesogenic GB elements in polymer systems with different spacer lengths ($m = 5$ and $m = 6$). Filled symbols, $\tau_{||}$; open symbols, $\tau_{\perp}$. For the GB model, we show the predictions of the analytical formulas 3 and 4 (solid lines) and Kramers expression (formula 5) for parallel orientational relaxation of planar rotator (dashed line).

difference leads (as will be discussed) to pronounced differences in orientational mobility for low-molecular weight and polymer LC compounds.

## IV. Orientational and Translational Mobility

To study orientational mobility we have calculated the orientational correlation functions, $P_{||}^{(1)}(t)$ and $P_{\perp}^{(1)}(t)$ defined in eqs 2, for Gay−Berne particles and bonds in the spacer (see Figure 10). These are the same functions investigated in ref 10. For the small-molecule system of unconnected GB units, these correlation functions decay exponentially over a rather wide time range. In the polymer systems, both for mesogenic elements in the polymer chain and for the spacer bonds, these functions are clearly nonexponential. This fact reflects the existence of a spectrum of relaxation times for the polymer chain.[26] To fit these dependencies, we use stretched exponentials $\exp\{-(t/\tau)^{\beta}\}$ where $\tau$ is a characteristic relaxation time, and $\beta$ is characteristic of the breadth of the relaxation spectrum. In the LC state, anisotropy of orientational mobility leads to two characteristic times $\tau_{||}$ and $\tau_{\perp}$. For unconnected GB molecules, we observe values of $\beta$ close to unity at all the temperatures studied in this work, corresponding to simple exponential decay. For the polymer systems, increased orientational ordering leads to a decrease in the value of $\beta$ (and hence an increase in the breadth of the spectrum of relaxation times associated with orientational relaxation) both for the GB units and the spacer bonds: for GB units $\beta$ falls from $\approx$0.6 to $\approx$0.4 while for the spacer bonds lower values are seen, falling from $\approx$0.3 to $\approx$0.2. These observations hold for all spacer lengths $m$ studied in this paper.

For the low molecular weight model, parallel relaxation times $\tau_{||}$ increase with increasing order parameter $S$, while perpendicular relaxation times $\tau_{\perp}$ decrease (see Figure 11). The dependence of perpendicular relaxation times is well described by eq 3 over a broad range of values of $S$. The analytical formulae, eqs 4 and 5, predict a much stronger variation of parallel relaxation time with $S$, especially in a well-ordered LC phase. Nevertheless, at intermediate values of order parameter (up to $S \approx 0.7$), relaxation times obtained in these MD experiments are in better agreement with eq 4, and, as a result, with the BD computer simulations of refs 10 and 14. The conclusion about the two main mechanisms of orientational motion made in ref 10 remains valid for this many-body system.

For the polymer model, orientational relaxation is much more complicated. Both parallel and perpendicular orientational relaxation times increase with ordering (see Figure 11). The difference in orientational relaxation between the low molecular weight GB system and the polymer can be explained by the pronounced increase in density (and decrease in free volume) of the polymer systems with ordering as compared to the liquid of unconnected GB molecules. This decrease of free volume strongly impedes both parallel and perpendicular orientational motions. For the low molecular weight GB system, the influence of ordering on density is rather small, and the resultant effect on the parallel and perpendicular relaxation times is similar to the motion of a single rigid dumbbell in an external quadrupole field.

The view, that the main effect on orientational mobility for the polymer LC is the decrease in free volume, is supported by comparing the orientational mobility of the mesogenic elements at the ends of the polymer chain with that in the middle. In spite of much more orientational mobility of the GB units at the ends, their parallel and perpendicular relaxation times both increase with increasing order. Ordering also leads to anisotropy of orientational mobility for the bonds in the flexible spacers. However, because of the small degree of orientational order, this anisotropy is less pronounced than that of the mesogenic elements.

It should be noted that the parallel orientational relaxation times for the polymer model become extremely long in the orientationally ordered phase, and our estimates of $\tau_{||}$ at the highest order parameters can only be approximate. This is not unexpected for highly elongated molecules: complete decay of $P_{||}^{(1)}(t)$ to zero will only happen on the timescale of complete molecular end-over-end rotation. This does not mean that other relevant properties of the ordered phase (for example, second-rank order parameters, stresses, etc.) are poorly equilibrated. Similar considerations apply, for instance, in the simulation of molecular solids.

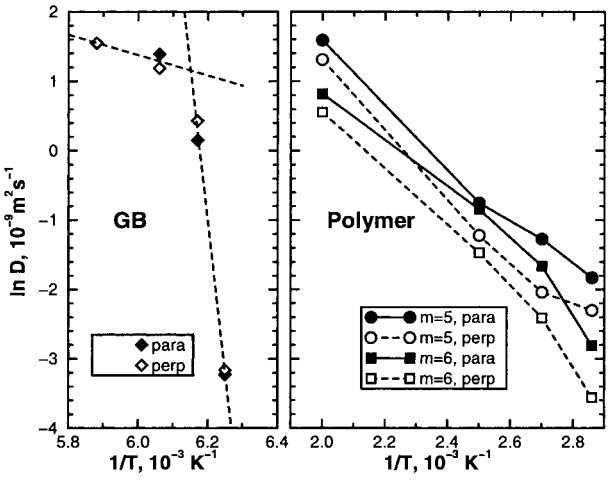


**Figure 12.** Parallel (filled symbols) and perpendicular (open symbols) translational diffusion coefficients for Gay−Berne liquid and for polymer systems with $m = 5$ and $m = 6$.

To study the local translational mobility of GB units in isotropic and LC states, we have calculated their mean-square translational displacements along the director $\langle \Delta r_{\parallel}^2(t) \rangle$ and in the perpendicular direction $\langle \Delta r_{\perp}^2(t) \rangle$. From the asymptotic slope of these dependences, the parallel and perpendicular translational diffusion coefficients $D_{\parallel}$ and $D_{\perp}$ have been calculated.

For the Gay−Berne system, both $D_{\parallel}$ and $D_{\perp}$ decrease with decreasing temperature and formation of the smectic phase. The difference of slope in their temperature dependence reflects the phase transition (see Figure 12). Interestingly, there is very little difference between $D_{\parallel}$ and $D_{\perp}$, even in the smectic phase.

For the polymer systems, translational mobility also decreases with ordering, both for parallel and perpendicular motion, but with different rates (and hence activation energies). The mean-square parallel displacement is higher than the perpendicular one (see Figure 12).

## V. Conclusions

In this paper we have reported the first results from extensive simulation studies of a family of main-chain polymer liquid crystal models. For a system of Gay−Berne units separated by flexible methylene spacer chains of various lengths $m$, we see the expected odd−even effects in the dependence of thermodynamic properties on $m$, and some evidence of such effects on the isotropic-liquid crystal transition temperature. Over the temperature range studied, the $m = 6$ system shows clear evidence of formation of a nematic phase below $T = 350$ K, and the $m = 8$ system has started to show orientational order. Nonetheless, the time scales for the ordering process are extremely long by comparison with those required for small-molecule systems, and the temperature range over which order develops is quite wide. For real LC polymers, the ordering temperatures are much more well-defined, and we have no explanation for this difference at present. Possibly, poor equilibration of our system is to blame, but we have allowed considerable periods of time for this (∼14 ns) and tested the system over further longer periods (∼8 ns) at the most important state points, without observing significant changes in the order parameter.

The density of the system (at the chosen pressure $P = 0$) changes significantly over the range $T = 350-500$ K studied here. This makes it difficult to specify the value of the density change at the nematic-isotropic transition: the density alters by 50−60% while the order parameter is changing from $S \approx 0.1$ to $S \approx 0.5$, but if we consider only the change from $S \approx 0.2$ to $S \approx 0.45$, the corresponding density increase is just a few percent. Experimentally, small changes of a few percent are observed.

The dynamical properties of the polymer chains are also qualitatively different from those of the analogous small-molecule system. While the pure Gay−Berne model shows roughly exponential decay of parallel and perpendicular first-rank orientational time correlation functions, which conform well to previously proposed theories for Brownian rotation in an external potential and the results of Brownian dynamics simulation, the analogous quantities for the mesogenic units in the polymer systems are well fitted by a *stretched* exponential form, the exponent of which is significantly different from unity. Both parallel and perpendicular relaxation times increase with increasing order parameter (and density) for the polymer systems; by contrast, in the small-molecule systems, the perpendicular relaxation time decreases with increasing order. In drawing comparisons between the different systems, we should not forget that the small-molecule Gay−Berne model orders to give a smectic-B phase (i.e., something close to a crystal) while the polymer models appear to be forming a much less structured nematic phase. Also, the polymer models order at a much higher temperature. Clearly, the connectivity in the polymer has a large effect on GB unit reorientation, so we should not expect the same theories to apply.

The translational motion of the polymers is also quite different in character from that of the small-molecule system. For GB molecules, a sharp change in activation energy occurs on passing through the isotropic−smectic transition. For this system, it happens that the parallel and perpendicular diffusion coefficients are similar to each other; naturally diffusion in the smectic phase is very slow. For the polymer systems, diffusion along the director (which means also substantially along the contour of the polymer chain) occurs much more readily than diffusion in the transverse direction. The effective activation energy for both processes varies continually with temperature; once more we should recall that substantial changes in density are occurring over the range studied here, and this undoubtedly affects the observed diffusion coefficients.

Direct comparison of our results with the real-life polymer liquid crystal series PE1/n, which was used to fix the molecular parameters, is not especially revealing. The experimental systems form smectic phases, while we have so far only observed a nematic phase in our simulations. This is not surprising, since we have made no attempt to construct a completely faithful model: our representation of the rigid core, for instance, completely neglects electrostatic forces and polarizability, and assumes axial symmetry. Our results should be taken as indicating the behavior of a simple, representative, system of rigid and flexible units: additional interaction terms may be added in a controlled way, and their effect on phase stability investigated, in the future. Ultimately, it should be possible to make direct, quantitative comparisons with specific systems, given sufficient investment of computer time.

In our work we have found it essential to use a parallel MD simulation algorithm running on massively parallel computers, in order to carry out runs of sufficient length to equilibrate and study these systems. Simulation timescales of the order of 10 ns seem to be essential. Our first results are only preliminary: they indicate that the model is capable of reproducing trends in experimentally observed behavior over a suitable range of temperature, and that further studies will be worthwhile. The results of such studies will be the subject of future publications.

**Acknowledgment.** This research was supported by EPSRC through the provision of computer hardware, a post-doctoral research assistantship for A.V.L., and computer facilities through the High Performance Computing Initiative. Use of computing resources at the Center for Scientific Computations (CSC) ESPO, Finland, is acknowledged. Funding from the Academy of Finland to I.N., and a postgraduate studentship for M.S.A.B. from the Sultan Qaboos University, Oman, are also gratefully acknowledged. We have had helpful discussions with T. M. Birshtein, Yu. Ya. Gotlib, and A. A. Darinskii. A.V.L. also gratefully acknowledges partial financial support from INTAS (Grant INTAS-93-2502 ext).

## References and Notes

(1) Wilson, M. R.; Allen, M. P. *Mol. Cryst. Liq. Cryst.* **1991**, *198*, 465.
(2) Wilson, M. R. *Mol. Phys.* **1995**, *85*, 193.
(3) de Miguel, E.; Martín del Río, E.; Brown, J. T.; Allen, M. P. *J. Chem. Phys.* **1996**, *105*, 4234.
(4) Allen, M. P.; Warren, M. A.; Wilson, M. R.; Sauron, A.; Smith, W. *J. Chem. Phys.* **1996**, *105*, 2850.
(5) Allen, M. P.; Warren, M. A. *Phys. Rev. Lett.* **1997**, *78*, 1291.
(6) Adams, D. J.; Luckhurst, G. R.; Phippen, R. W. *Mol. Phys.* **1987**, *61*, 1575.
(7) de Miguel, E.; Rull, L.; Gubbins, K. *Phys. Rev. A* **1992**, *45*, 3813.
(8) Perera, A.; Ravichandran, S.; Moreau, M.; Bagchi, B. *J. Chem. Phys.* **1997**, *106*, 1280.
(9) Darinskii, A.; Gotlib, Y.; Lukyanov, M.; Lyulin, A.; Neelov, I. *Prog. Colloid Polym. Sci.* **1993**, *91*, 13.
(10) Darinskii, A.; Lyulin, A.; Neelov, I. *Makromol. Chem. Theor. Sim.* **1993**, *2*, 523.
(11) Maier, W.; Saupe, A. *Z. Naturforsch* **1958**, *13*, 564.
(12) Meier, G.; Saupe, A. *Mol. Cryst.* **1966**, *1*, 515.
(13) Dozov, I.; Kirov, N. *J. Chem. Phys.* **1989**, *90*, 1099.
(14) Lyulin, A. V.; Darinsky, A. A.; Gotlib, Y. Y. *Phys. A* **1992**, *182*, 607.
(15) Kramers, H. *Phys.* **1940**, *7*, 284.
(16) Gay, J. G.; Berne, B. J. *J. Chem. Phys.* **1981**, *74*, 3316.
(17) Bilibin, A. Y.; Tenkovtsev, A. V.; Prianer, O. N.; Pashkovsky, E. E.; Skorokhodov, S. S. *Makromol. Chem.* **1985**, *186*, 1575.
(18) Ober, Ch. K.; Jin, J. I.; Lenz, R. W. *Makromol. Chem. Rapid Commun.* **1983**, *4*, 49.
(19) Frosini, V.; De Petris, S.; Chielini, E.; Galli, G. *Mol. Cryst. Liq. Cryst.* **1983**, *93*, 232.
(20) Shilov, V. V.; Dmitruk, N. V.; Goihman, A. Sh.; Skorokhodov, S. S.; Bilibin, A. Yu. *Vysokomol. Soedin, Ser B.* **1987**, *29*, 627.
(21) Cleaver, D. J.; Care, C. M.; Allen, M. P.; Neal, M. P. *Phys. Rev. E* **1996**, *54*, 559.
(22) Ryckaert, J.-P.; Bellemans, A. *Chem. Phys. Lett.* **1975**, *30*, 123.
(23) Fincham, D. *Daresbury Lab. Inf. Q. Mol. Dyn. Monte Carlo Simul.* **1984**, *12*, 47.
(24) Wilson, M. R.; Allen, M. P.; Warren, M. A.; Sauron, A.; Smith, W. *J. Comput. Chem.* **1997**, *18*, 478.
(25) Shilov, S.; Birshtein, T.; Volchek, B. *Makromol. Chem. Theor. Sim.* **1993**, *2*, 21.
(26) Gotlib, Y. Y.; Darinsky, A. A.; Svetlov, Y. Y. *Physical Kinetics of Macromolecules*; Chimia; Leningrad, 1986 (in Russian).

MA971105Y